INL/EXT-14-33252

Summary of BISON Development Activities NEAMS FY14 Report

R. L. Williamson
S. R. Novascone
J. D. Hales
B. W. Spencer
G. Pastore
D. S. Stafford
W. Liu
J. Ortensi
K. A. Gamble
D. M. Perez

October 2014

The INL is a U.S. Department of Energy National Laboratory
operated by Battelle Energy Alliance

Idaho National Laboratory

INL/EXT-14-33252

Summary of BISON Development Activities NEAMS FY14 Report

R. L. Williamson
S. R. Novascone
J. D. Hales
B. W. Spencer
G. Pastore
D. S. Stafford
W. Liu[1]
J. Ortensi
K. A. Gamble
D. M. Perez

[1]ANATECH, Inc.

October 2014

Idaho National Laboratory
Idaho Falls, Idaho 83415

http://www.inl.gov

Prepared for the
U.S. Department of Energy
Office of Nuclear Energy
Under DOE Idaho Operations Office
Contract DE-AC07-05ID14517

Summary of BISON Development Activities
NEAMS FY14 Report

[1]R. L. Williamson
[1]S. R. Novascone
[1]J. D. Hales
[1]B. W. Spencer
[1]G. Pastore
[1]D. S. Stafford
[2]W. Liu
[1]J. Ortensi
[1]K. A. Gamble
[1]D. M. Perez

[1]Idaho National Laboratory
[2]ANATECH, Inc.

Fuel Modeling and Simulation
Idaho National Laboratory
P.O. Box 1625
Idaho Falls, ID 83415-3840

October 1, 2014

Contents

1 Introduction

The objective of the NEAMS ToolKit is to develop a "pellet-to-plant" simulation capability useful for predicting performance and safety for a broad range of nuclear reactor power systems. The NEAMS ToolKit has been organized into a Fuels Product Line (FPL) and a Reactor Product Line (RPL) and is modular in design. Within the FPL, a multiscale approach has been adopted in which simulations of fuel performance at the engineering scale are informed by material property and irradiation performance models developed from mesoscale simulations of microstructural evolution. The focus in this report is on development and validation of the engineering-scale fuel performance analysis tool within the FPL, which is BISON [1].

This summary report contains an overview of work performed under the work package entitled "FY2014 NEAMS INL-Engineering Scale Fuel Performance & Interface with RPL Tools." A first chapter identifies the specific FY-14 milestones, providing a basic description of the associated work and references to related detailed documentation. Where applicable, a representative technical result is provided. A second chapter summarizes substantial additional work including 1) efforts to improve numerical convergence and contact in BISON, 2) development of capability to simulate hydrogen behavior in Zircaloy cladding and 3) efforts to enhance collaborative work with the Halden Research Program. A final chapter briefly outlines planned future work.

2 Milestone Summary

2.1 Milestone level and completion schedule

FY-2014 Milestones and the completion dates are listed in Table 2.1. Following sections contain a short description of each milestone and references to related detailed documentation. Where applicable, a representative technical result from the work is included.

Table 2.1: FY-2014 Milestones for NEAMS INL-Engineering Scale Fuel Performance Effort

Milestone	Completion Date	MS Level
Release BISON update for LWR fuel performance in quasi-steady state and off-normal conditions.	9/30	M2
Issue update to BISON validation and assessment report	9/30	M2
Issue BISON verification and validation plan	3/31	M2
Extend smeared cracking capability to 3D	2/28	M3
Modify material model design to generally allow multiple coupled nonlinear material models	4/30	M3
Enhance coolant channel model to include boiling curve, departure from nucleate boiling, and re-flood/quench capability	6/30	M3
Complete FUMEX-II and III priority cases for assessment effort	8/28	M3
Support development and coupling to depletion tool in MAMMOTH	9/30	M3

2.2 Release BISON update for LWR fuel performance in quasi-steady state and off-normal conditions

The major accomplishment for this year was the release of an updated version of BISON (Version 1.1) with corresponding documentation including an updated user [2] and theory manual [3]. The major new or improved capabilities in Version 1.1 include:

- Enhanced coolant channel model to handle the full boiling curve
- High temperature Zircaloy creep model for LOCA behavior
- Zircaloy high temperature microstructure phase change

- Transient fission gas release
- Improved hydrogen diffusion/precipitation models for Zircaloy
- Ability to generally allow multiple nonlinear material models
- Improved mechanical contact
- Improved thermal contact
- Three-dimensional smeared cracking behavior

BISON was also recently migrated to a new code repository (GitLab) and configuration management tool (git). This new approach provides the development team with a mechanism to review, approve or disapprove, and document all changes to the BISON source code.

2.3 Issue update to BISON validation report

The BISON Light Water Reactor (LWR) validation base was significantly enlarged by including priority cases from the FUMEX-II [4] and FUMEX-III [5] international coordinated research projects. The new cases are described in more detail below. All cases considered to date are documented in an updated BISON Validation report [6].

2.4 Issue BISON Verification and Validation plan

A detailed Software Verification and Validation plan for BISON was issued in March 2014 [7]. The document is organized into sections describing 1) software quality assurance, 2) code verification, 3) code validation and 4) code uncertainty quantification. Examples of verification and validation processes are summarized here.

2.4.1 Verification

Rather strict code verification practices are enforced within the BISON development process. Developers are responsible for developing regression tests for all of the code they develop. This helps ensure that future code changes do not break existing functionality. Some tests exercise the interaction of various models, and many others are single-feature verification tests.

By way of example, consider the process followed to introduce a new thermal conductivity model for UO_2 fuel. Having identified the particular form of the model (the mathematical description), the developer can identify the inputs to the model (e.g., temperature) as well as the outputs (thermal conductivity). The developer creates a test that will exercise the new model. This test will require specific boundary conditions and perhaps other carefully controlled inputs in order to produce the exact results expected through an independent, analytic calculation.

The developer must of course also encode the relevant equations in the BISON software and compile the new code. Having done so, the developer exercises the new capability on the new test. If the computed thermal conductivity does not match the analytic expression, the developer

searches for errors in the code and in the test until the discrepancy is resolved. Note that more than one verification test may be, and often is, required to give confidence that the encoded model is mathematically correct.

It should be understood that much of the underlying software in use by BISON has its own set of verification tests. In particular, verification tests concerned with the correctness of the finite element formulation are maintained at the MOOSE and libMesh levels.

BISON has many verification tests, checking solid mechanics, heat conduction, gap heat transfer, material models, mechanical contact, thermal contact, large strain capabilities, boundary conditions, plenum pressure determination, output, and many other phenomena needed for nuclear fuel analysis. That these tests run properly is evidence that the models have been implemented correctly.

A review of several of BISON's verification tests, along with an overview of verification in the context of nuclear fuel performance software in general and of BISON in particular, is in [8].

2.4.2 Validation

Since BISON is being developed as an "all fuels" code, the validation chapter within the Verification and Validation plan contains separate sections for LWR fuel, TRISO particle fuel and metallic fuel.

As an example, the document provides a detailed plan for validating BISON for LWR fuel using the following list of physical phenomena for which we have experimental measurements:

1. Beginning-of-life fuel centerline temperature (BOL FCT)
2. Ramp-test fuel centerline temperature (Ramp FCT)
3. Through-life fuel centerline temperature (TL FCT)
4. Through-life rod internal pressure (TL Press)
5. End-of-life fission gas release (EOL FGR)
6. End-of-life fuel grain size (EOL Grain Size)
7. End-of-life rod free volume (EOL Volume)
8. End-of-life fuel pellet density (EOL Density)
9. End-of-cycle cladding diameter change (EOC Cladding Dia)
10. End-of-cycle cladding waterside oxide thickness (EOC Oxide)
11. Fuel stack elongation (Fuel Elong)
12. Rod length change (Cladding Elong)

The cases considered to date are summarized in Tables 2.2, 2.3, 2.4, which are organized according to the previous list of measured quantities: fuel centerline temperature (FCT) at beginning of life (BOL), throughout life (TL) and during power ramps (Ramps), fission gas release (FGR), cladding outer diameter following pellet cladding mechanical interaction (Cladding Dia), and cladding elongation (Cladding Elong). Many of these assessment cases were chosen due to participation in the IAEA sponsored FUMEX Coordinated Research Projects and are priority cases from either FUMEX-II [4] or FUMEX-III [5]. Other cases were chosen based on recommendations from nuclear fuel experts. Some FUMEX-II and III cases were not selected as part of this year's validation efforts due to insufficient data, or if the experiment was considered low priority. Also note that the same experiments are listed in 2.3, and 2.4 because each of these tables show different experimental measurement categories.

Table 2.2: Summary table of BISON LWR assessment cases.

Experiment	Rod	BOL FCT	Ramp FCT	TL FCT	EOL FGR	EOC Cladding Dia	Cladding Elong
IFA-431	1,2,3	X					
IFA-432	1,2,3	X					
IFA-513	1,6	X		X			
IFA-515.10	A1	X					
IFA-597.3	7,8		X				X
Risø-3	AN3,AN4		X		X		
AREVA					X		
FUMEX-II	27(1,2a-d)				X		
Risø-3	GE7				X		
OSIRIS	J12					X	
REGATE					X	X	
PWR 16x16	TSQ002			X	X	X	
IFA-431 (3D)	4	X					

Table 2.3: Prioritized summary table for areas 1-6.

Experiment	Rod	BOL FCT	Ramp FCT	TL FCT	TL Press	EOL FGR	EOL Grain Size
US PWR 16x16	TSQ022			X	X	X	
IFA-534.14	18				X	X	X
IFA-534.14	19				X	X	X
HBEP	BK363					X	X
HBEP	BK365					X	X
HBEP	BK370					X	X
R. E. Ginna	2				X	X	
R. E. Ginna	4				X	X	
OSIRIS	H09					X	
Risø-3	II5		X		X	X	
Risø-3	II3		X		X	X	X
Risø-3	GE-m		X		X	X	X
IFA-535.5/6	809				X	X	
IFA-535.5/6	810				X	X	
Risø-3	AN2					X	X
TRIBULATION	BN1/3					X	
TRIBULATION	BN1/4					X	
TRIBULATION	BN1/15					X	

Table 2.4: Prioritized summary table for areas 7-12

Experiment	Rod	EOL Volume	EOL Density	EOC Cladding Dia	EOC Oxide	Fuel Elong	Cladding Elong
US PWR 16x16	TSQ022			X	X	X	
IFA-534.14	18	X			X		
IFA-534.14	19	X			X		
HBEP	BK363				X		
HBEP	BK365				X		
HBEP	BK370				X		
R. E. Ginna	2				X	X	
R. E. Ginna	4				X	X	
OSIRIS	H09	X	X	X	X	X	X
Risø-3	II5	X		X	X		X
Risø-3	II3	X		X	X		
Risø-3	GE-m			X	X		
IFA-535.5/6	809	X					X
IFA-535.5/6	810	X					X
Risø-3	AN2	X			X		
TRIBULATION	BN1/3	X		X		X	X
TRIBULATION	BN1/4	X		X		X	X
TRIBULATION	BN1/15	X		X		X	X

2.5 Extend smeared cracking capability to 3D

In ceramic fuel such as UO2, a significant temperature gradient develops from the fuel center to the radial edge. This gradient appears early and is strong enough to induce cracking in the fuel due to the accompanying stress. The cracks reduce the stress in the fuel and increase the effective fuel volume (decrease the gap size). A smeared cracking model in BISON may be invoked to account for this cracking. A smeared cracking model adjusts the elastic constants at material points as opposed to introducing topographic changes to the mesh, as would be the case with a discrete cracking model. When the smeared cracking model is active, principal stresses are compared to a critical stress. If the material stress exceeds the critical stress, the material point is considered cracked in that direction, and the stress is reduced significantly. From that point on, the material point will have no strength unless the strain becomes compressive. Two simple examples are shown here to demonstrate the capability. Demo 1, regression test: A single solid element is pulled uniformly in each of the axial directions in sequence. A stress vs. time plot is shown for each of the loadings in Figure 2.1.

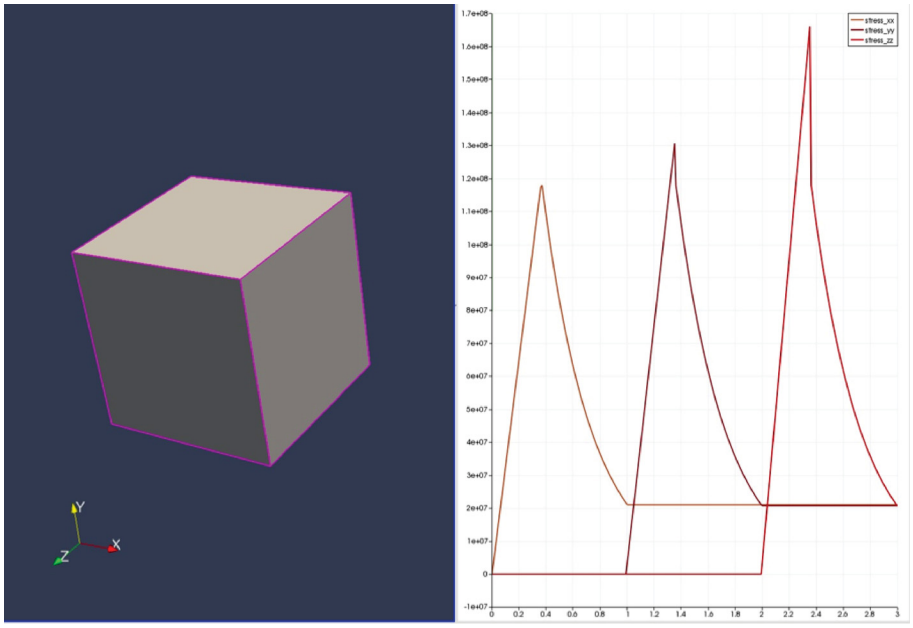

Figure 2.1: Stress response with smeared cracking behavior.

The stress rises linearly until the critical value is reached. After the critical value is reached, the stress relaxes according to a given function, and then remains constant at a predetermined value. Figure 2.1 shows this behavior for each of the three directions independently. Demo 2, simply supported composite beam with uniform pressure load: Results from a second 3D simulation are shown here to demonstrate a more practical example. In this example, a uniform pressure load is applied to the top surface of a composite beam that is simply supported. The

outside of the beam is concrete and the center is steel. This simulation was run two times. In the first example, the concrete is not allowed to crack. The top image in Figure 2.2 shows a contour of stress in the x-direction. In Figure 2.2, the images are of half the beam (cut longitudinally) and only show the concrete. The lower image of Figure 2.2 shows a contour of x-direction stress from a simulation where the concrete material was allowed to crack. Notice that the stress levels are much lower in the cracked beam. This is expected behavior and demonstrates that cracking occurs in the direction corresponding to the load, which means the model can represent cracks in three dimensions. We plan to use this feature in fuel performance simulations in hopes of more accurately representing the behavior of the fuel.

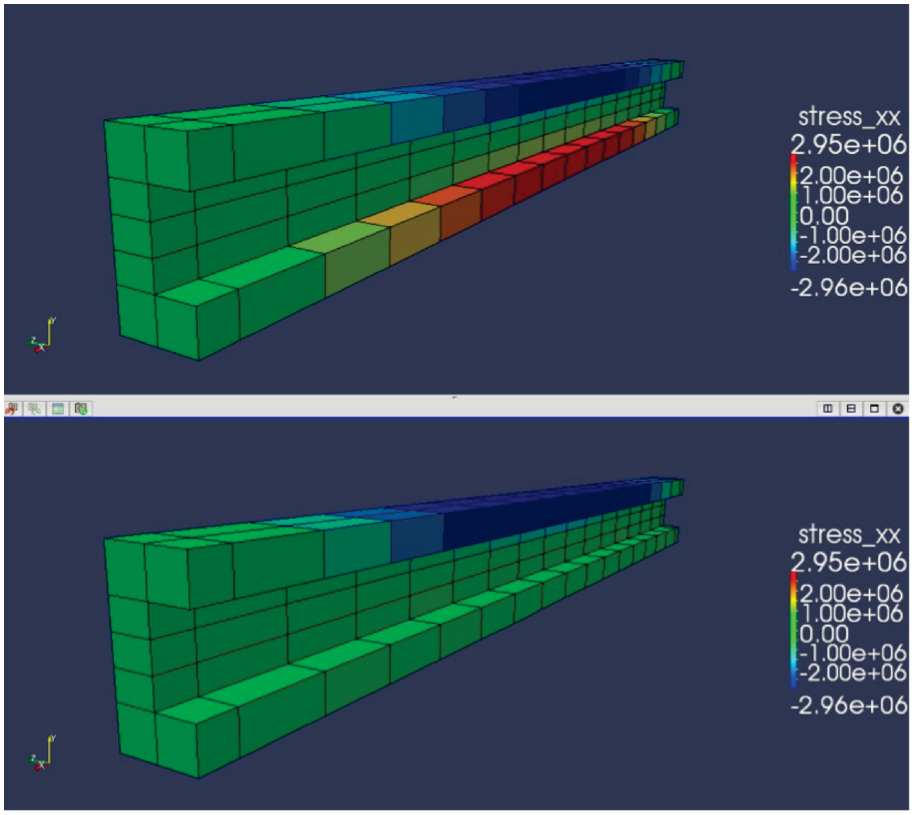

Figure 2.2: Stress response with smeared cracking behavior.

2.6 Modify material model design to generally allow multiple coupled nonlinear material models

Our approach to capturing the response from multiple nonlinear solid mechanics material models was updated. It is now much easier to use two or more models that are applied to one domain.

For example, the cladding can be represented by a thermal creep model and an instantaneous plasticity model. While this capability has always existed in BISON, the design and coding of such models is easier, with a more rigorous criteria for converging the material state between two or more nonlinear models. This makes running simulations to compare cladding diameter results easier and more robust.

In our approach, the creep and the instantaneous plasticity model are represented as specialized isotropic nonlinear materials. The creep model runs at an integration point, computing stress, elastic strain, and inelastic strain. The stress and strain are then given to the instantaneous plasticity model as inputs, and an update set of stress and strain is computed. The process repeats until the change in stress between iterations is below a specified tolerance.

When creep and instantaneous plasticity models are implemented according to the approach developed here, they may be combined through options in the input file. This greatly increases the flexibility of using combined creep and plasticity while simultaneously lowering the effort required to create such a combined material law.

To verify this capability, consider Example 3 from [9]. The problem is a one-dimensional bar which is loaded from yield to a value of twice the initial yield stress and then unloaded to return to the original stress. The bar must harden to the required yield stress during the load ramp, with no further yielding during unloading. The initial yield stress (σ_0) is prescribed as 20 with a plastic strain hardening of 100. The mesh is a 1x1x1 cube with symmetry boundary conditions on three planes to provide a uniaxial stress field. The temperature is held constant at 1000.

In the PowerLawCreep model, the creep strain rate is defined by:

$$\dot{\varepsilon} = A\sigma^n \times \exp^{(-Q/(RT))} \times t^m. \tag{2.1}$$

The creep law specified in the paper, however, defines the creep strain rate as

$$\dot{\varepsilon} = A_o m_o \times \sigma^n \times t^{(mo-1)} \tag{2.2}$$

with the creep parameters given by

$$\begin{aligned} A_o &= 10^{-7} \\ m_o &= 0.5 \\ n &= 5. \end{aligned}$$

Thus, input parameters for the test were specified as

$$\begin{aligned} A &= A_o m_o = 0.5 \times 10^{-7} \\ m &= m_o - 1 = -0.5 \\ n &= 5 \\ Q &= 0. \end{aligned}$$

The variation of load P with time is:

$$P = 20 + 20t \qquad 0 < t < 1.0 \tag{2.3}$$
$$P = 40 - 40(t-1) \qquad 1 < t < 1.5 \tag{2.4}$$

The analytic solution for total strain during the loading period $0 < t < 1$ is

$$\begin{aligned}\varepsilon_{tot} =& (\sigma_0 + 20t)/E + 0.2t \\ &+ At^{0.5}\sigma_0^n \left[1 + (5/3)t + 2t^2 + (10/7)t^3 + (5/9)t^4 + (1/11)t^5\right]\end{aligned} \tag{2.5}$$

and during the unloading period $1.0 < t < 1.5$

$$\begin{aligned}\varepsilon_{tot} =& (\sigma_1 - 40(t-1))/E + 0.2 + (4672/693)A\sigma_0^n \\ &+ A\sigma_0^n \left[t^{0.5}(32 - (80/3)t + 16t^2 - (40/7)t^3 \right. \\ &\left. + (10/9)t^4 - (1/11)t^5) - (11531/693)\right]\end{aligned} \tag{2.6}$$

where σ_1 is the stress at time t = 1.

Assuming a Young's modulus (E) of 1000 and using the parameters defined above,

$$\varepsilon_{tot}(1.0) = 2.39734$$
$$\varepsilon_{tot}(1.5) = 3.16813.$$

The numerically computed solution is

$$\varepsilon_{tot}(1.0) = 2.39826 \qquad (\sim 0.04\% \text{ error})$$
$$\varepsilon_{tot}(1.5) = 3.15663 \qquad (\sim 0.36\% \text{ error})$$

2.7 Enhance coolant channel model to include boiling curve, departure from nucleate boiling, and re-flood/quench capability

In the operating conditions of Light Water Reactors, fuel rods are surrounded by flowing water coolant, which carries the thermal energy generated through fission and transfers the heat into a steam generator or drives a turbine directly. To predict the performance of a fuel rod, heat transfer to the surrounding coolant is to be described in order to accurately determine the thermal boundary condition at the cladding outer wall. In the BISON code, such aspect of fuel rod modeling is handled by a dedicated coolant channel model. Correlations are implemented in this model for the heat transfer coefficient from cladding to coolant under different boiling and phase regions during normal and off-normal reactor conditions. Figure 2.3 shows how the heat flux changes as the wall temperature is increased (boiling curve). The different boiling regions and corresponding heat transfer correlations available within the BISON coolant channel model are specified. A variety of correlations that describe nucleate boiling conditions (both sub-cooled and saturated boiling) is available in BISON [3]. During off-normal reactor conditions (such as design-basis accidents), the heat flux may exceed the the critical heat flux (CHF). Above the

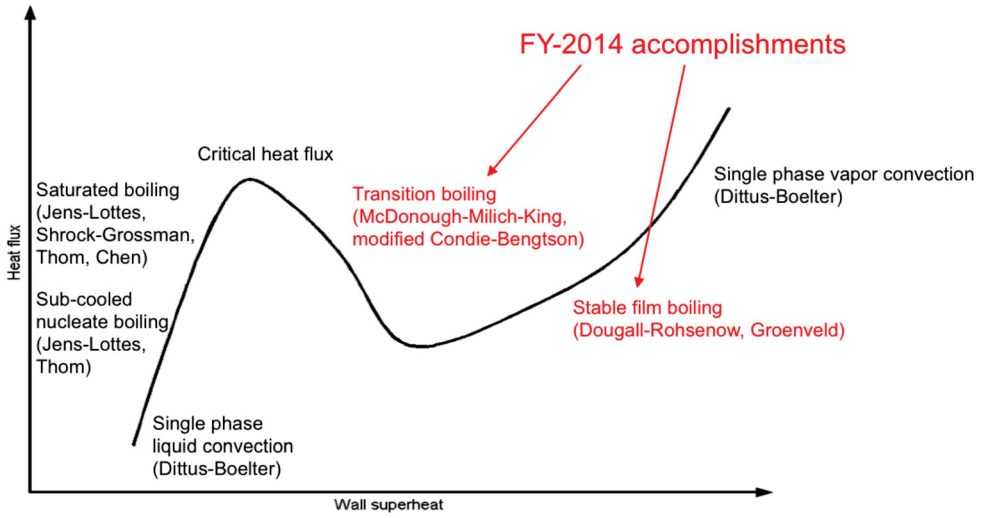

Figure 2.3: Boiling curve for water and correlations for heat transfer from cladding to coolant implemented in BISON.

CHF, the cladding outer surface is enclosed by vapor film and the heat transfer regime departs from nucleate boiling. The post-CHF heat transfer regime is divided into transition boiling and film boiling (Fig. 2.3).

During FY-2014, the BISON coolant channel model has been improved to allow for off-normal reactor conditions, by including departure from nucleate boiling. To this end, several correlations have been newly incorporated, which allow one to calculate the CHF as well as to describe heat transfer from cladding to coolant in the post-CHF boiling regions. Specifically:

- To calculate the CHF, a new correlation based on Zuber's hydrodynamic model [10] has been implemented. Other correlations for the CHF are also available within the BISON coolant channel model [3].
- To describe heat transfer from cladding to coolant during transition boiling regime, two correlations have been implemented, i.e., the McDonough-Milich-King [11, 12] and the modified Condie-Bengtson [12] correlations.
- For the film boiling regime, which occurs when the cladding wall temperature reaches the minimum film boiling temperature, the Dougall-Rohsenow [13, 12] and Groenveld [11, 12] correlations have been implemented.

In addition to the above code enhancements, an alternative approach to modeling heat transfer during a LOCA accident has been implemented, which provides a re-flood/quench capability. Such newly implemented approach consists of applying the empirical correlations from the FLETCH tests [14, 15] within the BISON coolant channel model. This set of correlations

permits to calculate the heat transfer coefficient from cladding to coolant during the re-flooding phase of a LOCA accounting for the movement of the quench front, which is missing in the approach based solely on the boiling curve The heat transfer coefficient is a function of flooding rate, cladding temperature and fuel rod power at the start of flooding, flooding water temperature, vessel pressure, elevation, and time [15].

More details on the implemented correlations are given in the cited references and in the BISON theory manual [3]. We intend to evaluate this model further in FY-2015, and use it for some simulations of fuel rod behavior during LOCAs.

2.8 Complete FUMEX-II and III priority cases for assessment effort

Tables 2.3 and 2.4 list the FUMEX priority [4],[5] cases that were simulated. These cases, along with the cases run previously (listed in Table 2.2) are documented in detail in the FY14 BISON Validation report [6].

2.9 Support development and coupling to depletion tool in MAMMOTH

The validation of MAMMOTH reactor physics is currently underway via the Benchmark for Evaluation and Validation of Reactor Simulations (BEAVRS). The FY14 work centered around the following tasks: 1) include better discretization of the reflector regions and peripheral structures in the 2-D and 3-D mesh, 2) add axial regions (supports, plenum, etc.) and grid spacers, 3) prepare higher fidelity cross sections using the DRAGON-5 MOC solver, and 4) perform comparisons to 2-D and 3-D reference Monte Carlo (MC) solutions and the benchmark for the Hot Zero Power (HZP) condition. The 2-D comparisons to the reference MC yield a -44 pcm difference in the eigenvalue and show very good agreement for the assembly powers with a root mean squared error of 0.532% and a maximum error of 1.32%. The detector signals show a root mean squared error of 1.15%, and a maximum error of 2.48%, when compared to MC. The result from the full 3-D model at HZP conditions was compared to the measured data provided in the benchmark. The calculated eigenvalue was 0.99994 and 1.00123, with and without grid spacers, respectively. This value is expected to decrease approximately 80 pcm, with better spatial convergence of the model. The all rods out isothermal temperature coefficients (ITC) were computed at the nominal temperature of 566K and at 10K above and below nominal. The ITC for the lower extend (-10K) was -1.73 pcm/F, the higher extend (+10K) was -2.50 pcm/F. The average ITC is, therefore, -2.12 pcm/F compared to the measured value of -1.75 pcm/F. The comparison to measured detector signals, shown in Figure 2.4, yield an root mean squared error of 4.00% and a maximum error of 9.8%. These results are quite good, if one takes into account that 1) OpenMC MC results had a root mean squared error of 5.4% and a maximum of 11% and 2) the model is based on average assembly enrichments and not with as-built enrichments. The main reason for the discrepancy in both the deterministic and MC models has to do with the significant radial tilt in the low power measurements, especially in assemblies with only one symmetric location. These comparisons will improve significantly at hot full power conditions.

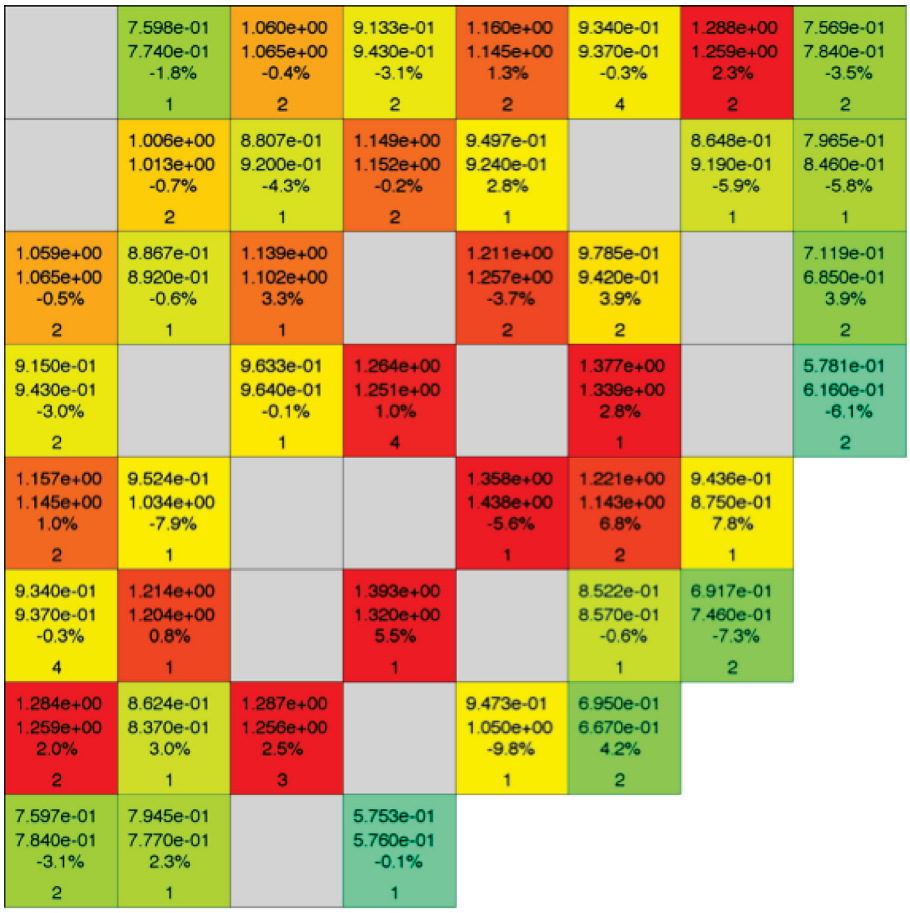

Figure 2.4: Comparison of the detector signals calculated vs measured at Hot Zero Power conditions.

3 Additional Accomplishments

3.1 Convergence and contact improvements

For BISON to be a useful tool for fuel simulations, it is extremely important for it to be able to robustly obtain a converged solution for the system of equations describing fuel behavior. BISON's solver robustness has generally been quite good before mechanical contact between the fuel and cladding occurs, but there have been significant challenges obtaining converged solutions once that contact occurs and the solver begins to enforce mechanical contact constraints. Significant development effort has been focused on the enforcement of mechanical contact to provide improved solution robustness.

The original implementation of mechanical contact enforcement in BISON and MOOSE is based on a system in MOOSE known as the `DiracKernel`, which is used to apply boundary conditions to a point. For the node on face, master/slave mechanical contact enforcement, two instances of `DiracKernel` are created: one for the slave side, to apply point loads at nodes, and one for the master side, to apply point loads at the locations on faces of the nodes on the opposing surface. This system correctly enforces the constraints, but it is limited because it does not provide the ability to fill in all of the off-diagonal entries in the Jacobian matrix used for preconditioning.

In the preconditioned Jacobian-free Newton Krylov (JFNK) algorithm used by BISON to solve the tightly coupled nonlinear equation system, a series of linear iterations are used to obtain each iterative update to the nonlinear solution in Newton's method. If a solution struggles to converge these linear iterations, it is often an indication of a poor preconditioner. That has typically been the case for BISON problems that experienced solution difficulties during contact enforcement. For that reason, the efforts to improve solution robustness with contact have been focused on improving the preconditioner.

A new system in MOOSE known as the `Constraint` system has been developed to permit improved and more flexible enforcements of arbitrary constraints between arbitrary solution variables at different nodes. The `Constraint` system can be used to enforce the same mechanical contact constraints that have traditionally been enforced using the `DiracKernel` system. The advantages of the `Constraint` system are that the same C++ class with code for enforcing contact can be used for both the master and slave sides of the interface, and that it permits the computation of the full set of terms in the Jacobian matrix. Providing a more complete set of these terms is expected to improve preconditioning, and hence, improve the robustness of the linear iterations.

The mechanical contact enforcement code has been re-implemented using the `Constraint` system. A more complete set of coupling terms has been implemented in this system. Both this new system and the original system are available to the user, and a single input file parameter can be used to switch between these systems. The new `Constraint`-based mechanical contact

enforcement algorithm has been tested on a number of models in the BISON test suite, and has resulted in significantly improved solution robustness in many of these cases. Multiple problems that previously would not converge now run to completion, and run times have been shortened on problems that previously did run to completion. The converged solutions are unchanged with the new system, as it enforces the same mathematical constraints on the equation system.

The preconditioning process consists of both of creating a matrix that is a good approximation of the Jacobian, and also of a method to apply that preconditioner to the solution. Direct solvers can be used to do this, but iterative solvers are often used for efficient, scalable parallel solutions. The preconditioning matrix calculated with the new contact enforcement algorithm results in greatly improved convergence on small problems where direct solvers are used to apply the preconditioner.

There are still challenges, however, with the iterative methods typically used to precondition larger BISON models. The algebraic multigrid (AMG) preconditioner that has been traditionally used on BISON models often does not converge as well with the `Constraint` system as it did with the `DiracKernel` system. It is believed that this is because of the way the AMG algorithm coarsens out degrees of freedom, and the way this interacts with contact nodes. Work is in progress to develop a way to split out the contact degrees of freedom into a separate system and precondition it separately from the rest of the problem. While the AMG preconditioner doesn't work as well with the new system, it has been found that an additive Schwartz method (ASM) works very well on most 2D problems with the new contact enforcement. This is the standard method currently being used for 2D problems.

The new `Constraint` system requires more memory usage than the `DiracKernal` system because of the additional terms in the preconditioner. While that has not been a severe issue for most 2D problems, this has limited its effectiveness for large 3D problems. Work is underway to address this issue by minimizing unnecessary entries in the Jacobian.

In summary, the developments this year have resulted in significant improvements in convergence robustness for 2D problems, and the new contact enforcement system is being regularly used for 2D models. Developments currently underway are expected to further improve the robustness and efficiency of solutions of models with contact in 2D, and enable the use of the new algorithms on 3D problems, which should provide robustness improvements similar to those already realized for 2D models.

3.2 Hydrogen behavior in Zircaloy cladding

Modeling hydrogen in Ziracloy is the subject of [16]. Many details of BISON's hydrogen modeling capability may be found there. Further work has occurred this year to revamp the hydride modeling in BISON, focusing on improving the quality of the implementation and removing issues with time stepping. As part of this work, the small time step restriction imposed by the original hydride model was removed. The upgrade enables large, multidimensional simulations to be run efficiently while still capturing hydrogen pickup, diffusion, precipitation, and dissolution.

In addition to verification cases, the hydride model has recently been validated against [17]. In this experiment, an initially uniform hydrogen distribution is redistributed in one dimension

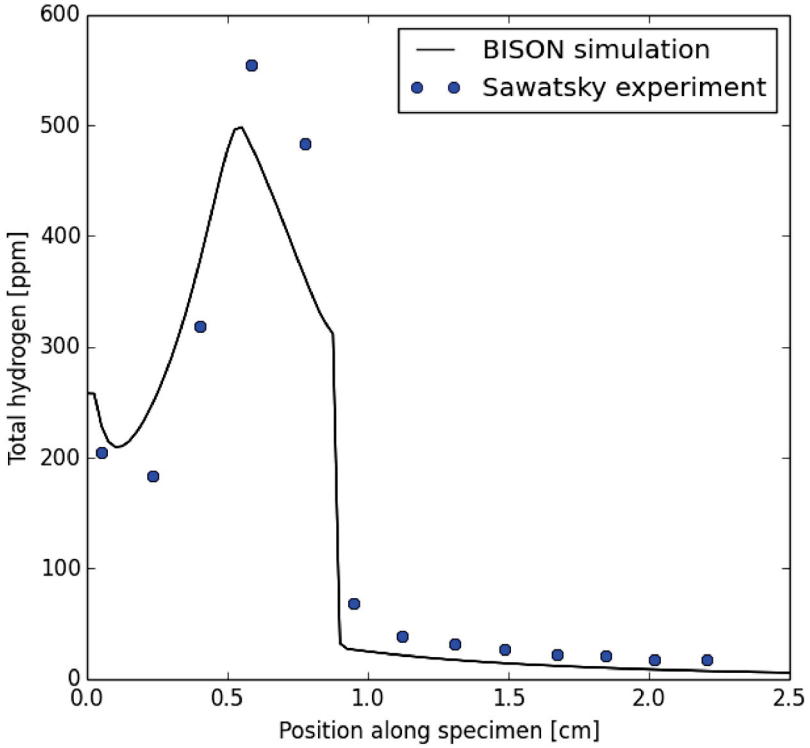

Figure 3.1: Validation of BISON hydride model against Sawatzky's 1D hydride redistribution experiment [17].

using a thermal gradient so that some hydrogen forms zirconium hydride at one end of the domain. Modeling this in BISON tests the Fickian diffusion, Soret diffusion, precipitation, and dissolution kernels (i.e. everything except for hydrogen pickup from the cladding). As shown in Figure 3.1, BISON predicts the major features of the experiment.

We have also begun work to simulate UFD scenarios that include hydride formation, beginning with high-burnup irradiation, continuing with cooling in the spent pool, and finishing with drying and long-term storage in casks. The model currently includes separate thermo-mechanical and precipitation models, which eases time stepping restrictions that the fully-coupled case would impose.

Thermal gradients in cladding lead to higher hydrogen concentrations at the outer cladding radius and in the vicinity of pellet-pellet interfaces. This effect can be seen in Figure 3.2.

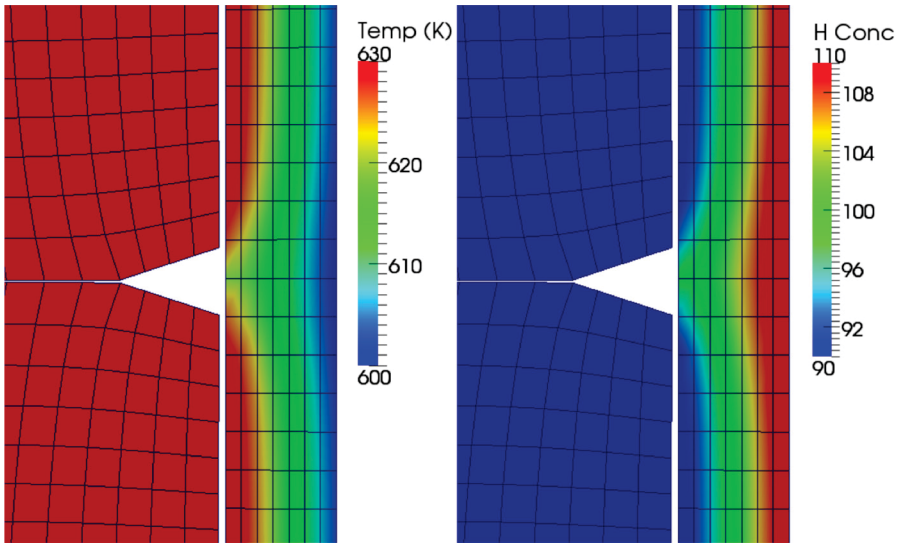

Figure 3.2: Temperature and hydrogen concentration in cladding near a pellet-pellet interface.

3.3 Collaboration with Halden Reactor Project

A large fraction of the LWR experimental data in the BISON validation base is from the Halden Reactor Project in Norway. Substantial additional data exists and is being evaluated for further validation work. Specifically, in recent years valuable data on fuel behavior during LOCAs has been measured and will be used in FY-15 to begin validation of accident analysis capabilities in BISON.

During FY-14 NEAMS funding was used to support enhancement of existing collaborative work between INL and the Halden Reactor Project. A BISON model of an upcoming experiment (IFA-744) has been developed and is being used to support experimental design. This experiment will provide accurate measurements of fuel thermal conductivity variation with temperature and burnup. Recent efforts involved investigation of the effects of both radial and circumferential fuel cracking, assuming the cracks are filled with either lead bismuth or helium (both potential materials filling the fuel-clad gap). Since very accurate fuel temperature measurements are required in this experiment, the effects of crack size and filling material were parametrically studied to determine their effect on fuel centerline temperature. As the experiment is run, measured and calculated temperatures will be compared in support of BISON validation activities.

Members of the BISON team also participated in the recent Enlarged Halden Program Group meeting, held every 18 months. Two papers were presented at the meeting, one concerning the IFA-744 effort described above [18] and the other documenting the recent development of a transient fission gas release model in BISON [19]. A meeting was held with Halden management to discuss further collaboration including experiments specifically designed to validate the 3D aspects of BISON. Discussions are also ongoing concerning enhancing our collaboration by having a member of the BISON team on temporary assignment at Halden.

4 Future Work

In 2015, the BISON team plans to improve convergence, expand accident simulation capability, initiate material model development for fast oxide fuels, and continue the validation effort.

New preconditioning approaches and solver (PETSc) development work are examples of tasks planned for increasing convergence performance. We plan to work closely with the PETSc team such that the BISON team becomes more familiar with using PETSc features and investigate ways in which interaction between these codes can be improved.

More precise treatment of fuel material and behavior models is planned. A more stable approach to smeared cracking shall be investigated and integration of smeared cracking, fuel creep, and stress-based densification models will be implemented.

Accident capabilities will be expanded. We first plan to do an extensive evaluation of the coolant channel model (developed in 2014) applied to LOCA scenarios. Also planned is the coupling via Multi-App Transfers of BISON to RELAP7. This coupling should result in a better representation of LOCA due to the two-phase flow capabilities in RELAP7. We will also begin gathering data for the purpose of validating LOCA capability.

Validating BISON against experimental measurements is an ongoing effort that will continue in 2015. An increase in full-length fuel rod simulations is planned. The number of validation cases that we consider will increase substantially when we convert ENIGMA validation case input files to BISON input files.

The long term vision of the NEAMS campaign is to build simulation capability for fast oxide fuels. We plan to implement thermal and mechanical (creep) models for MOX (30%PU) fuel and investigate methods to model central void formation.

The BISON team will provide user support throughout the year via the bison-user group email list, training sessions, and updates to documentation.

Bibliography

[1] R. L. Williamson, J. D. Hales, S. R. Novascone, M. R. Tonks, D. R. Gaston, C. J. Permann, D. Andrs, and R. C. Martineau. Multidimensional multiphysics simulation of nuclear fuel behavior. *J. Nucl. Mater.*, 423:149–163, 2012.

[2] J. D. Hales, S. R. Novascone, G. Pastore, D. M. Perez, B. W. Spencer, and R. L. Williamson. BISON users manual. Technical report, Idaho National Laboratory, September 2014.

[3] J. D. Hales, S. R. Novascone, G. Pastore, D. M. Perez, B. W. Spencer, and R. L. Williamson. BISON theory manual: The equations behind nuclear fuel analysis. Technical report, Idaho National Laboratory, September 2014.

[4] IAEA. Fuel Modelling at Extened Burnup (FUMEX-II): Report of a Coordinated Research Project 2002-2007. Technical Report IAEA-TECDOC-1687, International Atomic Energy Agency, 2002-2007.

[5] IAEA. Improvement of Computer Codes Used for Fuel Behaviour Simulation (FUMEX-III): Report of a Coordinated Research Project 2008-2012. Technical Report IAEA-TECDOC-1697, International Atomic Energy Agency, 2008-2012.

[6] D. M. Perez, R. L. Williamson, S. R. Novascone, G. Pastore, J. D. Hales, and B. W. Spencer. Assessment of BISON: A nuclear fuel performance analysis code. Technical report, Idaho National Laboratory, September 2014.

[7] BISON software V and V plan. Technical Report INL/EXT-14-31671, Idaho National Laboratory, July 2014.

[8] J. D. Hales, S. R. Novascone, B. W. Spencer, R. L. Williamson, G. Pastore, and D. M. Perez. Verification of the BISON fuel performance code. *Ann. Nuclear Energy*, 71:81–90, September 2014.

[9] Paul Duxbury, Tony Crook, and Paul Lyons. A consistent formulation for the integration of combined plasticity and creep. *Internat. J. Numer. Methods Engrg.*, 37:1277–1295, 1994.

[10] L. S. Tong and Y. S. Tang. *Boiling Heat Transfer and Two-phase Flow*. Taylor & Francis, Washington, D.C., USA, 2nd edition, 1997.

[11] N. E. Todreas and M. S. Kazimi. *Nuclear Systems I: Thermal Hydraulic Fundamentals*. Hemisphere Publishing Corporation, New York, N.Y., USA, 1990.

[12] Fuel Analysis and Licensing Code: FALCON MOD01 – Volume 1: Theoretical and Numerical Bases. Technical Report EPRI-1011307, December 2004.

[13] R. L. Dougall and W. M. Rohsenow. Film boiling on the inside of vertical tubes with upward flow of the fluid at low qualities. Technical Report MIT 9079-26, 1963.

[14] F. F. Cadek, D. P. Dominicis, H. C. Yeh, and R. H. Leyse. Pwr flecht final report supplement. Technical report, October 1972.

[15] M. E. Cunningham, C. E. Beyer, P.G. Medvedev, and G. A. Berna. FRAPTRAN: A Computer Code for the Transient Analysis of Oxide Fuel Rods. Technical Report NUREG/CR-6739 Vol.1, PNNL-13576.

[16] Olivier Courty, Arthur T. Motta, and Jason D. Hales. Modeling and simulation of hydrogen behavior in Zircaloy-4 fuel cladding. *J. Nucl. Mater.*, 452:311–320, 2014.

[17] A. Sawatzky. Hydrogen in zircaloy-2: Its distribution and heat of transport. *Journal of Nuclear Materials*, 2(4):321 – 328, 1960.

[18] J. D. Hales, P. G. Medvedev, S. R. Novascone, D. M. Perez, and R. L. Williamson. Analysis of double-encapsulated fuel rods. In *Enlarged Halden Programme Group Meeting*, Roros, Norway, September 7–12 2014.

[19] G. Pastore, D. Pizzocri, J. D. Hales, S. R. Novascone, D. M. Perez, B. W. Spencer, R. L. Williamson, P. Van Uffelen, and L. Luzzi. Modeling of transient fission gas behavior in oxide fuel and application to the BISON code. In *Enlarged Halden Programme Group Meeting*, Roros, Norway, September 7–12 2014.